

Limits of the equivalence of time and ensemble averages in shear flows.

Yuhong Wang, Kapilanjan Krishan, and Michael Dennin

Department of Physics and Astronomy, University of California at Irvine, Irvine, California 92697-4575

(Dated: January 26, 2020)

In equilibrium systems, time and ensemble averages of physical quantities are equivalent due to ergodic exploration of phase space. In driven systems, it is unknown if a similar equivalence of time and ensemble averages exists. We explore effective limits of such convergence in a sheared bubble raft using averages of the bubble velocities. In independent experiments, averaging over time leads to well converged velocity profiles. However, the time-averages from independent experiments result in distinct velocity averages. For comparison, ensemble averages are approximated by randomly selecting bubble velocities from independent experiments. Increasingly better approximations of ensemble averages converge toward a unique velocity profile. Therefore, the experiments establish that in practical realizations of non-equilibrium systems, temporal averaging and ensemble averaging can yield convergent(stationary) but distinct distributions. This provides strong evidence that a single realization of the experiment can reach a well-defined steady-state without exploring all of phase space.

PACS numbers: 05.20.Gg,05.70.Ln,83.80.Iz

A central tenant of statistical mechanics is the ergodic hypothesis: during time evolution, thermodynamic systems pass through almost all possible microstates leading to the equivalence of time and ensemble averages [1, 2, 3, 4, 5]. The exploration of phase space is achieved through thermal fluctuations, and this property of equilibrium systems has been used extensively. Its utility derives from the fact that it allows for a description of equilibrium dynamics in terms of well defined averaged observables. The observables are extracted either by averaging over states explored over long periods of time or from ensembles of states distributed over all of phase space, whichever method is most convenient for the observable being studied. The utility of the ergodic hypothesis in equilibrium systems naturally raises the question of whether or not athermal fluctuations in a driven system lead to the equivalence of time and ensemble averages through a similar exploration of phase space.

An ideal test of the equivalence of time and ensemble averages in driven systems would require measuring the instantaneous value of an observable for an infinite period of time for temporal averaging, and constructing an infinite number of ensembles representing different points in phase space to develop an ensemble average. This is untenable for real experiments; however, if time scales of observation are faster than intrinsic timescales, it is possible to gather a reasonable approximation of the distribution of values for an observable. An ensemble of independent states is approximated by performing the experiment multiple times with independent and uncorrelated initial conditions.

One expects any differences that exist between time and ensemble averaging to be related to the fundamental nature of microscopic fluctuations. In driven, complex fluids, athermal fluctuations arise through nonlinear particle rearrangements that are induced by flow. The potential for these athermal fluctuations to play a role

that is similar to thermal fluctuations in normal fluids is the basis of many statistical treatments of highly non-equilibrium complex fluids. In this paper, we investigate the ability of athermal fluctuations in the system to explore phase space in a manner that results in an equivalence between time and ensemble averages. When such equivalence exists, one can use well developed statistical techniques for extracting average properties of the fluid.

In considering any comparison of time and ensemble averages, it is important to recognize the separate question of the *convergence* of either time or ensemble averages. Independent of whether the two averages agree, it is possible that the nature of athermal fluctuations in a driven system are such that average quantities are not well-defined on experimentally accessible time scales or number of ensembles. This is highlighted by work in granular matter in which extremely long times were required for convergence of the average density under tapping [6]. As we will demonstrate, for our system, both the time and ensemble averages are well-defined.

In this Letter, we report on measurements of the average velocity profile using a model two-dimensional foam: a bubble raft [7]. One advantage of using a foam is that thermal fluctuations are essentially irrelevant. Aqueous foam consists of bubbles of gas separated by liquid walls. Under an applied constant rate of strain, the initial response of the foam is for the bubbles to stretch elastically. Eventually, bubbles undergo neighbor switching events, referred to as T1 events, that enable flow. These T1 events, and the associated bubble rearrangements, result in fluctuations in the stress, energy, and bubble positions [8]. The interesting feature is that despite the highly nonlinear and irregular nature of individual T1 events, the long time average of the bubble velocities is usually well defined. The average velocity profile for foam has been the subject of substantial theoretical [9, 10, 11, 12] and experimental [13, 14, 15, 16, 17, 18] work in regard to

developments in effective temperatures, jamming, shear localization, etc. However, the connection between time and ensemble averages for velocity profiles in foam (and other complex fluids) remains an open question.

The bubble raft is produced by flowing regulated nitrogen gas through a needle into a homogeneous solution of 80% by volume deionized water, 15% by volume glycerine, and 5% by volume Miracle Bubbles (from Imperial Toy Corporation). The bubbles are confined between two parallel bands separated by a distance d . The bands are driven at a constant velocity v_w in opposing directions. This applies a steady rate of strain to the system given by $\dot{\gamma} = 2v_w/d$. The total applied strain is $\gamma = \dot{\gamma}t$, where t is the time interval under consideration. The direction of flow imposed by the bands is taken to be parallel to the x-axis. We use a CCD camera to capture the state of the system at a frame rate fast enough to resolve individual T1 events. These events correspond to the fastest dynamical process occurring during shear. Each image of the system thus corresponds to a measurement of its instantaneous state. A Particle Image Velocimetry program [19] is then used to extract velocities of individual bubbles using consecutive images. The bubbles are relatively monodisperse, with a bubble diameter of $D = 2.66 \pm 0.2$ mm. Details of the apparatus and methods can be found in Ref. [20].

It is critical to define the distributions of bubble velocities that are used in the averaging process. First, for each separate time run, $N = 1000$ images are taken. For each image, a central region of the system is selected for averaging. In this region, the y-direction is divided into 40 distinct bins, and the x-component of velocities (for ease of notation, we will use v to denote the x-component of the velocity) for all of the bubbles in each bin is computed. There is approximately 20 bubbles per bin. In what follows we use i to denote each bubble, $t = 1, 2, \dots, 1000$ to denote the image (this is the discrete version of time), and j for the bin (this is the discrete version of the y coordinate). We use $r = 1, 2, \dots, 10$ to indicate the particular experimental run. For the ensemble averages, we use $e = 1, 2, \dots, 10$ to denote the particular ensemble used for averaging. Therefore, the velocity of a bubble is denoted by $v_r^i(j, t)$ (or $v_e^i(j, t)$) where $1 \leq t \leq N$, $1 \leq j \leq 40$, and $1 \leq r \leq 10$ (or $1 \leq e \leq 10$). The average velocity profile for each run is $v(y) = \langle v_r^i(t, j) \rangle_{i,t}$, where $\langle \rangle_{i,t}$ indicates that an average over all the bubbles in bin j for the entire time t of run r .

The only difference between each run was the initial configuration of the bubble in the system; all other parameters were fixed. This difference was exploited to generate approximate ensemble averages. The basic procedure consisted of selecting M time runs to create a set bubble velocities $v_e^i(j, t^*)$, where $1 \leq t^* \leq Mt$ is the new image index for this set of images. From this set of velocities, for each bin j , $N = 1000$ images are randomly selected to average over. This produces an approxima-

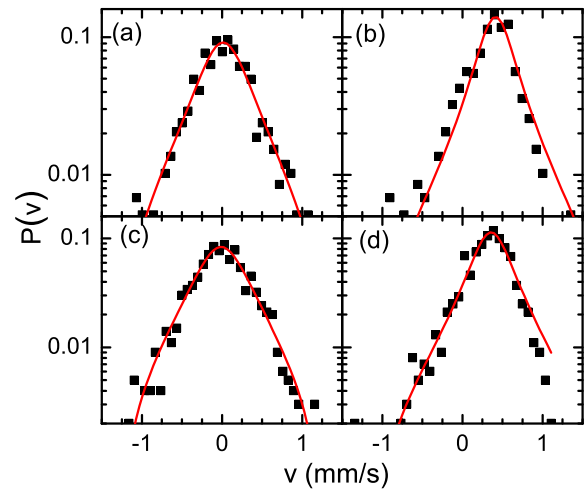


FIG. 1: (color online) The probability distribution of velocities is indicated for ensemble averaging (a, b) and time averaging (c, d) toward the center of the trough (a, c) and off center in bin number 10 (b, d). The solid lines are Lorentzian fits to the data.

tion of the ensemble average using the same number of images as was used for the time averages. For most of the following discussion, $M = 10$, and all of the separate runs were used to generate the ensembles. It should be noted that this method only approximates an ensemble average because we expect some correlations to remain between images in a single time run, and by construction, the “ensemble” has multiple images from the same time run in it.

Figure 1 provides examples of the distributions of velocities used for both time and ensemble averages (using $M = 10$) for two different bins. In both cases, the distributions have long tails that are consistent with a Lorentzian. This had been reported earlier for time averages [21]. The interesting feature is that our ensembles also appear to be consistent with Lorentzians, with no obvious difference from the time distribution except for a shift of the central value in off-center bins.

Because the velocity profiles under these conditions are extremely close to linear [20], individual profiles are best distinguished by plotting the difference between the profile and a linear profile (v_L). This is illustrated in Fig. 2 using the average velocity in all 40 bins ($v(y)$) for five realizations of a time average and five ensemble averages (using $M = 10$). In the case of time averaging, the resulting average velocity profiles clearly differ from each other. In contrast, the ensemble averages are essentially indistinguishable from each other. It is interesting to note that there still remains a systematic deviation from a linear profile for this level of approximation to an ensemble av-

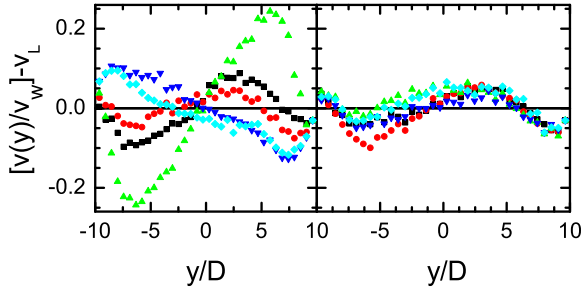


FIG. 2: (a) Deviation of mean velocity (normalized by the wall speed v_w) from a linear profile (v_L) generated by five different experimental realizations. (b) Deviation of five different ensemble averages of the velocities from a linear profile. Plotting the deviation highlights the differences between the different time average profiles. In contrast, the ensemble averages are relatively indistinguishable. The y-position is scaled by the bubble diameter D .

erage. Also, for both the time and ensemble averages, the deviation from a linear profile is significantly smaller than deviations as a function of other external parameters, such as the use of a top plate [20]. The source of these small deviations is outside the scope of this letter, and it will be the subject of future research.

Given the variation in time averages, it is important to understand the convergence of each average measurement. In Fig. 3, the convergence of the mean velocity as a function of the number of images (or bubbles) used to compute the average is plotted. For time averages, this corresponds to increasing the total time (or strain) used to compute the average. There are two key features. First, in all cases (ensemble and time averages), the mean values have converged to a well-defined value after averaging over approximately $n = 2000$ bubbles. Second, the spread in the final mean values is very different for the two methods [22]. For the time averages, as expected from Fig. 2, the deviation in final mean values is larger than the fluctuation in the mean for large enough values of n . For the ensemble averages, the deviation in final mean values is similar to the fluctuation in the mean. To quantify this concept, we define the deviation $\delta \equiv v_{max} - v_{min}$, where v_{max} (v_{min}) is the largest (smallest) final average velocity.

Clearly, using only ten runs is expected to be a relatively small “ensemble”. Though using significantly more runs is experimentally prohibitive, we verify the progression of convergence to a unique profile as the ensemble is constructed from sampling across an increasing number of uncorrelated experimental runs. In Fig. 4, the amount of convergence is parameterized by $\delta(M)$, where δ is as defined in Fig. 3. The parameter M corresponds to the number of runs used to generate the ensemble. For each

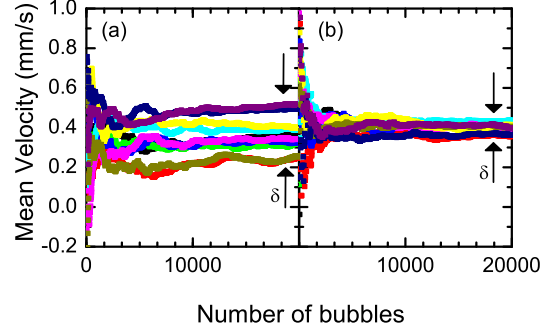


FIG. 3: (color online) (a) The mean values of the velocity in bin number 10 computed using time averaging. (b) The mean values of the velocity in bin number 10 computed using ensemble averaging. In both cases, the mean value is plotted as a function of the number of bubbles used to compute the average. The deviation in these values (indicated by the arrows and δ) is larger for time averages in comparison to ensemble averages.

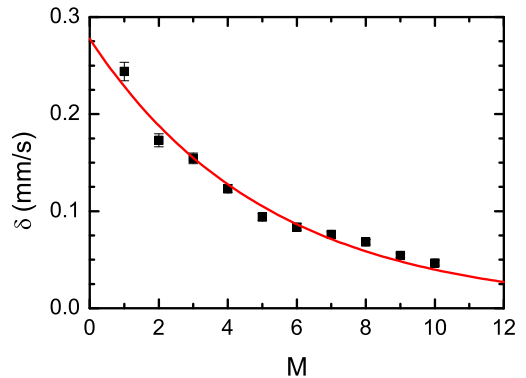


FIG. 4: (color online) Plot of the deviation δ between different realizations of average velocities as a function of M , the number of runs used to generate the ensemble. As the size of the ensemble increases, the deviation between computed averages decreases. The solid line is a fit to an exponential.

$1 \leq M \leq 10$, we randomly select M of the time runs to form an ensemble. Then, we compute the average velocity in bin 10 using $N = 1000$ images. We repeat this process ten times for each value of M , and then compute the deviation δ between the ten realizations. For example, for $M = 3$, we use an “ensemble” constructed from three runs that have been randomly selected from our original ten runs. This ensemble is used to compute one average velocity profile by randomly selecting $N = 1000$ images. Next, we select a new set of three runs and repeat the process ten times. Finally, once we have computed

δ for this set of ten realizations, we repeat the process thirty times, generating thirty values of δ for each M . The results of the average values of δ as a function of M are given in Fig. 4. Note, $M = 1$ represents the deviation between the original 10 runs. The solid line in Fig. 4 is a fit to an exponential ($\delta(M) = (0.28 \text{ mm/s})e^{-M/5.1}$). Referring back to Fig. 2, the value of the decay constant is consistent with the small deviation between the approximate ensemble average and a linear profile. Furthermore, the fit of $\delta(M)$ to an exponential suggests that the true infinite ensemble limit is linear.

These experiments show that athermal fluctuations during flow produce well-defined time-averaged velocity profiles that are not unique. Figure 3 illustrates how the final state of the system varies strongly with the initial bubble configuration. This suggests that bubble fluctuations during flow do not provide sufficient exploration of phase space to produce time-averaged velocity profiles that are independent of initial conditions. These different profiles are nonlinear in nature (see Fig. 2). In contrast, ensemble averaging results in convergence to a single profile which is substantially closer to linear. This confirms that the limit of time averaging is different from that of ensemble averaging for this system, on relevant *experimental* time scales.

It should be noted that an important feature in the experiment is that the temporal averaging is dominated by athermal fluctuations. In many mesoscopic driven systems, the fluctuations induced by external forcing is co-existent with thermal fluctuations, and the purely athermal effects are difficult to study. In these experiments, we were able to focus on athermal fluctuations because thermal fluctuations are not relevant to the bubble raft. Therefore, it is interesting to consider previous connections between microscopic nonlinearities leading to chaos and mechanisms of ergodicity [23]. The present study indicates that the nonlinearities associated with athermal fluctuations actually lead to a breakdown of ergodic behavior because of insufficient exploration of phase space.

These results have important implications for two current areas of research in complex fluids: proposals for effective temperatures [24, 25, 26] and the proposed jamming paradigm [27, 28]. A number of definitions of effective temperatures have been proposed [29]; however, quantitative agreement among them remains elusive [30]. Our results suggest that this disagreement may be connected to the fact that athermal fluctuations do not provide sufficient exploration of phase space for certain variables, such as velocity. For the jamming transition, simulations support the existence of a special point (the J-point) in the jamming phase diagram that has features of a phase transition [31]. However, the role of fluctuations in the jamming transition and distinctions between thermal and athermal fluctuations in this context still need to be clarified, and issues of ergodicity will impact these considerations.

This work was supported by a Department of Energy grant DE-FG02-03ED46071. The authors thank Corey O'Hern and Manu for useful discussions.

- [1] L. Boltzmann, *Wiener Berichte* **63**, 712 (1871).
- [2] L. Boltzmann, *Nature* **51**, 413 (1895).
- [3] L. Boltzmann, *Nature* **52**, 221 (1895).
- [4] L. D. Landau and E. M. Lifshitz, *Statistical Physics (Third Edition), Part 1* (Butterworth-Heinemann, Oxford, 1980).
- [5] R. K. Pathria, *Statistical Mechanics(Second Edition)* (Butterworth-Heinemann, Oxford, 1996).
- [6] E. R. Nowak, J. B. Knight, E. Ben-Naim, H. M. Jaeger, and S. R. Nagel, *Phys. Rev. E* **57**, 1971 (1998).
- [7] L. Bragg and W. M. Lomer, *Proc. R. Soc. London, Ser. A* **196**, 171 (1949).
- [8] D. Weaire and S. Hutzler, *The Physics of Foams* (Clarendon Press, Oxford, 1999).
- [9] F. Varnik, L. Bocquet, J.-L. Barrat, and L. Berthier, *Phys. Rev. Lett.* **90**, 095702 (2003).
- [10] N. Xu, C. S. O'Hern, and L. Kondic, *Phys. Rev. Lett.* **94**, 016001 (2005).
- [11] A. Kabla and G. Debrégeas, *Phys. Rev. Lett.* **90**, 258303 (2003).
- [12] D. Weaire, E. Janiaud, and S. Hutzler, *cond-mat* p. 0602021 (2006).
- [13] P. Coussot, J. S. Raynaud, F. Bertrand, P. Moucheront, J. P. Guilbaud, H. T. Huynh, S. Jarny, and D. Lesueur, *Phys. Rev. Lett.* **88**, 218301 (2002).
- [14] J. Lauridsen, G. Chanan, and M. Dennin, *Phys. Rev. Lett.* **93**, 018303 (2004).
- [15] G. Debrégeas, H. Tabuteau, and J. M. di Meglio, *Phys. Rev. Lett.* **87**, 178305 (2001).
- [16] A. D. Gopal and D. J. Durian, *J. Colloid. Interf. Sci.* **213**, 169 (1999).
- [17] F. Rouyer, S. Cohen-Addad, M. Vignes-Adler, and R. Höhler, *Phys. Rev. E* **67**, 021405 (2003).
- [18] B. Dollet, F. Elias, C. Quilliet, C. Raufaste, M. Aubouy, and F. Gruner, *Phys. Rev. E* **71**, 031403 (2005).
- [19] Detailed description of method and code is available at <http://www.physics.uci.edu/~foams>.
- [20] Y. Wang, K. Krishan, and M. Dennin, *Phys. Rev. E* **73**, 031401 (2006).
- [21] Y. Wang, K. Krishan, and M. Dennin, *Phys. Rev. E* **74**, 041405 (2006).
- [22] For Lorentzian distributions, the standard deviation is not well-defined; therefore it is not possible to estimate errorbars on the mean values. In fact, the mean values will fluctuate due to contributions from the tails of the distributions.
- [23] P. Cvitanović, R. Artuso, R. Mainieri, G. Tanner, and G. Vattay, *Chaos: Classical and Quantum* (Niels Bohr Institute, Copenhagen, 2005).
- [24] L. F. Cugliandolo, J. Kurchan, and L. Peliti, *Phys. Rev. E* **55**, 3898 (1997).
- [25] I. K. Ono, C. S. O'Hern, D. J. Durian, S. A. Langer, A. J. Liu, and S. R. Nagel, *Phys. Rev. Lett.* **89**, 095703 (2002).
- [26] L. Berthier and J.-L. Barrat, *Phys. Rev. Lett.* **89**, 095702 (2002).

- [27] A. J. Liu and S. R. Nagel, *Nature* **396**, 21 (1998).
- [28] V. Trappe, V. Prasad, L. Cipelletti, P. N. Segré, and D. A. Weitz, *Nature* **411**, 772 (2001).
- [29] F. Zamponi, F. Bonetto, L. F. Cugliandolo, and J. Kurchan, *J. of Stat. Mech. - Theory and Exp.* p. P09013 (2005).
- [30] C. S. O'Hern, A. J. Liu, and S. R. Nagel, *Phys. Rev. Lett.* **93**, 165702 (2004).
- [31] C. S. O'Hern, L. E. Silbert, A. J. Liu, and S. R. Nagel, *Phys. Rev. E* **68**, 011306 (2003).
- [32] D. M. Mueth, G. F. Debreygas, G. S. Karczmar, P. J. Eng, S. R. Nagel, and H. M. Jaeger, *Nature* **406**, 385 (2000).
- [33] W. Losert, L. Bocquet, T. C. Lubensky, and J. P. Gollub, *Phys. Rev. Lett.* **85**, 1428 (2000).
- [34] D. Howell, R. P. Behringer, and C. Veje, *Phys. Rev. Lett.* **82**, 5241 (1999).
- [35] J.-B. Salmon, A. Colin, S. Manneville, and F. Molino, *Phys. Rev. Lett.* **90**, 228303 (2003).
- [36] P. A. Thompson and G. S. Grest, *Phys. Rev. Lett.* **67**, 1751 (1991).
- [37] S. Y. Liem, D. Brown, and J. H. R. Clarke, *Phys. Rev. A* **45**, 3706 (1992).
- [38] N. Xu, C. S. O'Hern, and L. Kondic, *Phys. Rev. E* **72**, 041504 (2005).